



The 8th International Conference on
Structural Health Monitoring of Intelligent Infrastructure
Brisbane, Australia | 5-8 December 2017

Satellite-Based Monitoring of a Highway Bridge in Canada - Challenges, Solutions and Value

D. Cusson¹, K. Trischuk¹, D. Hébert², G. Hewus³, M. Gara⁴, P. Ghuman⁴

¹ National Research Council Canada – Canada, Email: daniel.cusson@nrc.gc.ca, ² Transport Canada – Canada,
³ Federal Bridge Corporation Limited - Canada, ⁴ 3v Geomatics - Canada

Abstract

An innovative space-borne bridge displacement monitoring technology was demonstrated on a major highway bridge in Cornwall (Canada) over a two-year period. Two major challenges had to be overcome and solutions were identified and implemented. The first challenge related to the proper selection and analysis of satellite imagery to optimize the number and signal quality of point targets on the bridge for adequate movement detection and analysis. The second main challenge was the comparison and validation of independent sets of data having different measurement methods, reference baselines, and distributions in space and time.

The key findings are as follows: (i) The regression analysis of Interferometric SAR (InSAR) data from the satellite produced the best coherence when fitted against three independent variables, being height, temperature, and time; (ii) The bridge railings appeared to be excellent SAR reflectors with their sharp edges and regular spacing along the bridge, showing a return of over 3,000 clear InSAR point targets to the satellite; (iii) The SAR displacement thermal sensitivity data was found to compare well to numerical modelling thermal data when computed along the longitudinal axis of the bridge. Results show great promise and value in applying satellite-based technology for the remote monitoring of highway bridges to optimize preventive maintenance management, extend structural lifespan, minimize traffic disruptions due to late repairs, and ensure structural integrity after extreme events such as major earthquakes and flooding.

1. Introduction

Highway bridges are critical to Canada's road transportation network and are in urgent need of rehabilitation, owing to ageing, limited capital investment, and insufficient inspection and maintenance. Bridge owners in North America have been struggling for decades with how to cost-effectively rehabilitate their large portfolios of highway bridges (U.S. DOT/FHWA/FTA 2007).

As a complement to current inspection and maintenance protocols, the judicious use of structural health monitoring (SHM) of highway bridges can contribute to addressing many of these challenges and slowing down the ageing of such critical structures. Preliminary studies (Marinkovic *et al.* 2007; Cusson *et al.* 2012) have shown that remote monitoring with radar satellites can provide ground measurements with sub-centimeter accuracy. The RADARSAT-2 Satellite, for instance, is capable of monitoring large structures by detecting and measuring movements on hundreds of point targets (PTs) on a single structure, while hundreds of these structures can be monitored and analysed in a single scene when acquired over major urban centres (Cusson *et al.* 2012).

The main objectives of this demonstration project were (i) to deploy a bridge displacement monitoring technology based on satellite imagery (Satellite Aperture Radar, or SAR) and (ii) to validate it against numerical bridge model predictions of thermal displacements, and measurements from displacement/temperature sensors installed on a highway bridge.

Figures 1-3 present the new 335 m long, 4-span, low-level North Channel Bridge (being the subject of this study) and the old high-level North Channel Bridge (being demolished at the time), crossing the St-Lawrence River between City of Cornwall (North) to Cornwall Island (South), located in Ontario, Canada. The new bridge was completed and opened to traffic in January 2014, while the demolition of the old steel bridge superstructure started in Sept. 2014 and ended in Nov. 2015.



Fig. 1: Drone view of the new low-level bridge and the old high-level bridge in Cornwall, ON



Fig. 2: View of bridges looking South (2015-09-15)



Fig. 3: View of bridges looking South-West (2015-10-21)

2. Acquisition Plan and InSAR Analysis of Satellite Imagery

Among the different modes of radar images that can be acquired with RADARSAT-2, the Spotlight mode is best-suited for bridge monitoring applications, which provides highest accuracy (but smallest coverage $\sim 18 \text{ km} \times 8 \text{ km}$). Anticipating possible image viewing issues given the complex configuration and timing of the construction/demolition work, four stacks of images from the Canadian Space Agency were requested, each with a repeat cycle of 24 days. For each ascending pass and each descending pass of the right-looking satellite, two stacks of images with low (26°) and high (47°) incidence angles were selected. Only one stack was to be retained for final analysis.

In an initial analysis, challenges related to proper selection of satellite imagery were addressed to optimize the number and stability of PTs for movement detection. These challenges included:

- Shadow effects – due to the positioning of the bridges (Fig. 1), with the upper structure creating SAR shadows on the lower structure's image, reducing the number of PTs (Ferretti *et al.* 2007);
- Layover effects – also due to the relative positioning of the bridges and the nature of SAR data collection, where the upper bridge can appear on the opposite side of the lower bridge depending on the viewing angle and the relative slant ranges of the bridges from the satellite, thus requiring additional processing of PTs to separate valid mixed targets (Ferretti *et al.* 2007);
- Target stability – due to construction activity on the bridges (e.g. cranes on new bridge, Fig. 2; and the gradual dismantling of the old bridge's steel superstructure, Fig. 3), reducing the number of valid consistently stable point targets for the final analysis;
- Multi-bounce effects – occurring when microwaves bounce off more than one physical object or entity (e.g. body of water) before returning to the SAR sensor, requiring additional processing or contributing to signal noise when mixed physical targets are not themselves stable;
- Height fit – as precise localization of point targets on the bridge requires accurate 3D positioning, which in turn requires derivation of an accurate estimate of each point target's height relative to a known digital elevation model (DEM). This can be a challenging task when there is a lot of variance in the data due to noise or unmodelled strong thermal effects.
- Number of scenes – where 12 to 15 valid scenes in a given stack are typically required to obtain sufficient measurement accuracy from an InSAR analysis of RADARSAT-2 satellite data.

The preliminary analysis revealed that, for the case at hand, the *sla74-asc* stack (ascending pass with a 26.5° incidence angle) was the most suitable stack for the subsequent detailed analysis.

For the full analysis, SAR data (radar wave phase information) were processed with a multi-model linear regression analysis to extract different sets of data from the *sla74-asc* imagery for over 3000 point targets registered on the new bridge deck. Key parameters included:

- Height (m) – fitted against perpendicular baseline (stereo sensitivity) data (Ferretti *et al.* 2007);
- Displacement thermal sensitivity ($\text{cm}/^\circ\text{C}$) – fitted against measured temperatures at the bridge;
- Displacement time rate (cm/year) – fitted against time from the first image acquisition;
- Coherence (ranging from 0 to 1) – confirming the quality of fit and the reliability of processed displacement data, where only PTs with coherence ≥ 0.8 should be trusted for InSAR analysis (Ferretti *et al.* 2007). The coherence is computed following a multi-model regression fit, yielding a statistic on both the quality of fit as well as the noise level of the point target.

A Python script was used to extract, de-noise, and visualize post-processed data by displaying displacement thermal sensitivity collected over the deck, as shown in Fig. 4 (X axis=West-East distance (reversed); Y axis=North-South distance; Z axis=Height). The figure reveals useful details:

- Displacement thermal sensitivity shows gradual variation along the bridge (more later);
- Height and slope of bridge deck (1.2° over 335 meters) are well captured by the point cloud;
- Steel railings returned a large amount of clear signals to the satellite. The sharp angles of the bridge railings appear to be excellent natural corner reflectors. Another advantage is that snow and ice do not accumulate easily on railings due to their exposure to wind and sun.
- Four groups of outliers leaning towards East appear to match exactly the locations of the four piers of the old bridge (East-West reversed), confirming exact positioning of the point cloud.

Figure 5 (left) presents the resulting displacement time rate data superposed onto a Google Earth optical image. With all points being either yellow or green, one can conclude that very small movements have occurred over the relatively short monitoring period. Figure 5 (right) illustrates the coherence of the displacement data over a Google Earth image, confirming the high quality and reliability of the processed data, with most points being dark blue (well above 0.8) – a coherence of 0.8 or higher on directional data is comparable to a standard deviation of less than 0.45 radians.

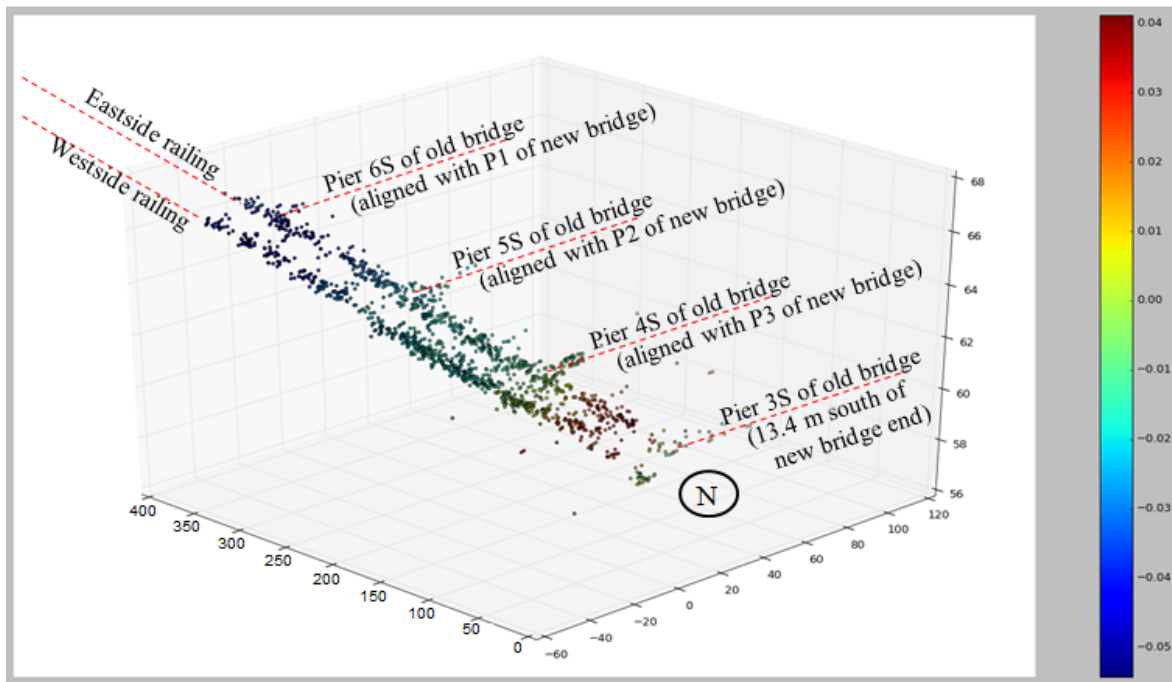


Fig. 4: 3D plot (m) of InSAR displacement thermal sensitivity data ($\text{cm}/^{\circ}\text{C}$)

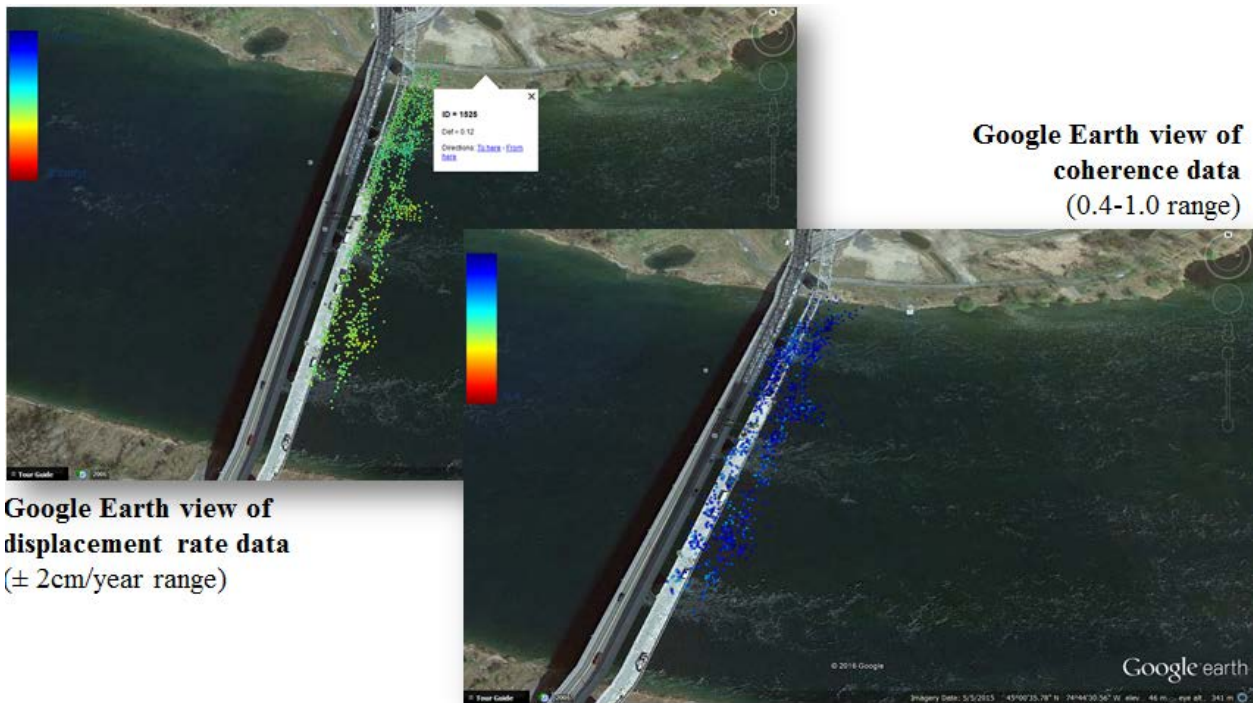


Fig. 5: Processed displacement time rate data (left) and corresponding coherence data (right)

3. Sensor-Based Bridge Monitoring

To validate the proposed satellite-based monitoring technology on the North Channel Bridge, the measurements from RADARSAT-2 need to be compared to similar measurements from other known ground-based technologies, including (i) temperature and displacement sensors installed on the bridge, and (ii) a finite-element numerical model of the bridge calibrated on sensors measurements from a truck load test.

3.1 Measurement of Ambient Conditions

Ambient temperature plays a crucial role in this study, as it is required in the proposed InSAR analysis of the satellite data, since our adopted approach is to fit the satellite displacement data with temperature data in order to remove the thermal movement and focus on mechanical movements of the bridge that could be due to settlement, problematic joints or bearing, excessive loading, etc.

A first set of temperature data was obtained from temperature sensors installed inside the twin steel box girders of the bridge, as shown in Figure 6. Being in direct contact with the steel girder, these sensors are expected to provide values similar to ambient air temperatures, due to the high thermal conductivity of steel. A second set of temperature data was obtained from the nearby Massena Intl. Airport's weather station (NY State, USA; 23 km away), as it was the closest station that could provide hourly values of air temperature. Using bridge temperature data over airport data to fit SAR displacement data resulted in a small improvement in measured coherence (not shown).

Figure 7 illustrates the correspondence between the bridge sensor temperatures and the Massena airport temperatures at different times, where each data point corresponded to the time of a satellite pass over the bridge. The strong correlation between the two sets of temperature data and the small improvement in observed coherence suggest that if sensor measurements are not available at the site being monitored, local airport temperatures are suitable for the proposed InSAR analysis approach.

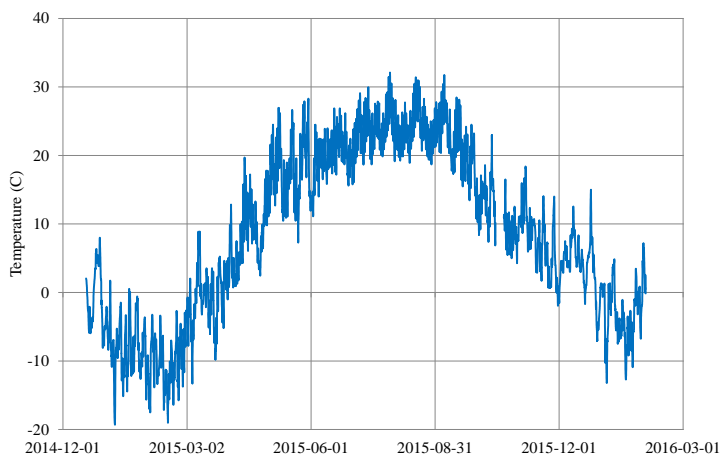


Fig. 6: Temperature measured inside steel box girder of bridge

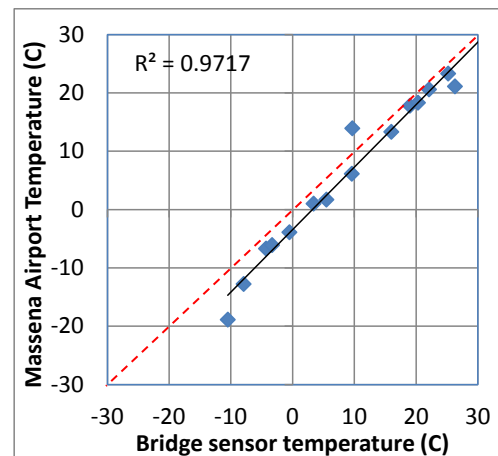


Fig. 7: Correspondence between bridge sensor temperature and local airport temperature

3.2 Measurement of Live Loads

Two truck load tests were conducted on February 2, 2016 during the evening (low traffic period), including a first test on the southbound (SB) lane and a second test on the northbound (NB) lane, with the 2nd last truck axle (Figure 8) aligned with mid-span position on Span 4 (first from North).

Wireless fiber-optic displacement sensors at the bottom of the twin steel box girders were used to measure the longitudinal deformations at the quarter-span and mid-span locations of Span 4. Figure 9 presents the deformations measured during the northbound lane test. It can be seen that the load test produced a horizontal elongation of 0.087 mm when the truck came into position, and an identical horizontal shortening when the truck left the bridge. Measurements from the two load tests were used to calibrate the finite-element model of the bridge by simulating identical load tests, comparing with the measurements, and adjusting Young's modulus of the reinforced concrete deck.



Fig 8: Truck used for load test on SB lane of bridge - Truck load=640 kN; Axle sp =4.3, 1.5, 6.5, 2.5, 1.5, 1.5 m

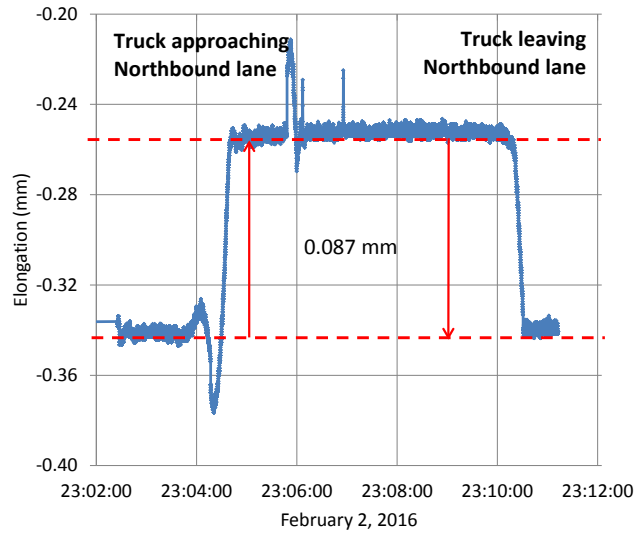


Fig 9: Load test data from mid-span sensor in East girder

4. Bridge Numerical Modelling

Since radar satellite sensing provides line-of-sight displacement measurements without distinguishing thermal effects from mechanical effects, or between the X, Y, and Z components of displacement, another tool is required to help determine the orthogonal components of mechanical effects on the bridge that could lead to structural issues if left undetected. This tool could be numerical modelling to determine the thermal movements of the bridge.

The commercial TNO-Diana finite element software package was used to build a detailed 3D numerical model of the North Channel Bridge in Cornwall, Ontario (steel-reinforced concrete deck on twin steel box girders). The construction drawings of the bridge and its construction specifications were used to obtain detailed information on bridge geometry, boundary conditions, and structural material properties. For a bridge under service loads, a structural static analysis and isotropic linear material models were deemed more than adequate for the determination of bridge displacements as a function of service loads and temperature effects.

Figure 10 illustrates the bridge model with the superstructure, three piers and two abutment walls (incl. 10,000 nodes, 11,154 elements, 6 materials, and 61 properties). The piers were modelled from their fixed connection to the superstructure down to their fixed connection to the river bed rock. The load-bearing portion of each abutment wall was modelled assuming uniaxial bearing connection (i.e. free movement in longitudinal direction, and blocked in transverse and vertical directions).

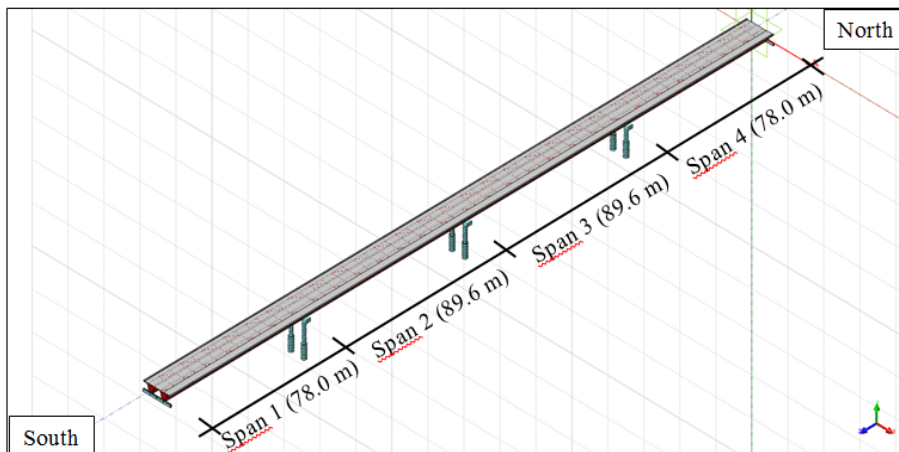


Fig 10: Overall view of complete 3D FE bridge numerical model

4.1 Numerical Model Calibration with Load Test Results

The truck load test conducted on the bridge on February 2, 2016 was simulated using a structural linear analysis of the bridge model for the 2 truck passes (SB and NB lanes). Figure 11 indicates the locations of the applied axle loads with the vertical black arrows, and those of the 4 wireless sensors on the steel box girders. After small adjustments to Young’s modulus of the deck’s reinforced concrete (set to 35 GPa), the longitudinal deformations of bottom layer of steel girders at mid-span and quarter-span compared well with sensor measurements. For example, at mid-span on SB lane (1st test), the predicted vs. measured values were 0.10 mm vs. 0.10 mm in the West girder, 0.08 mm vs. 0.07 mm in the East girder; and at mid-span on NB lane (2nd test), the predicted vs. measured values were 0.09 mm vs. 0.07 mm in the West girder, and 0.11 mm vs. 0.09 mm in the East girder.

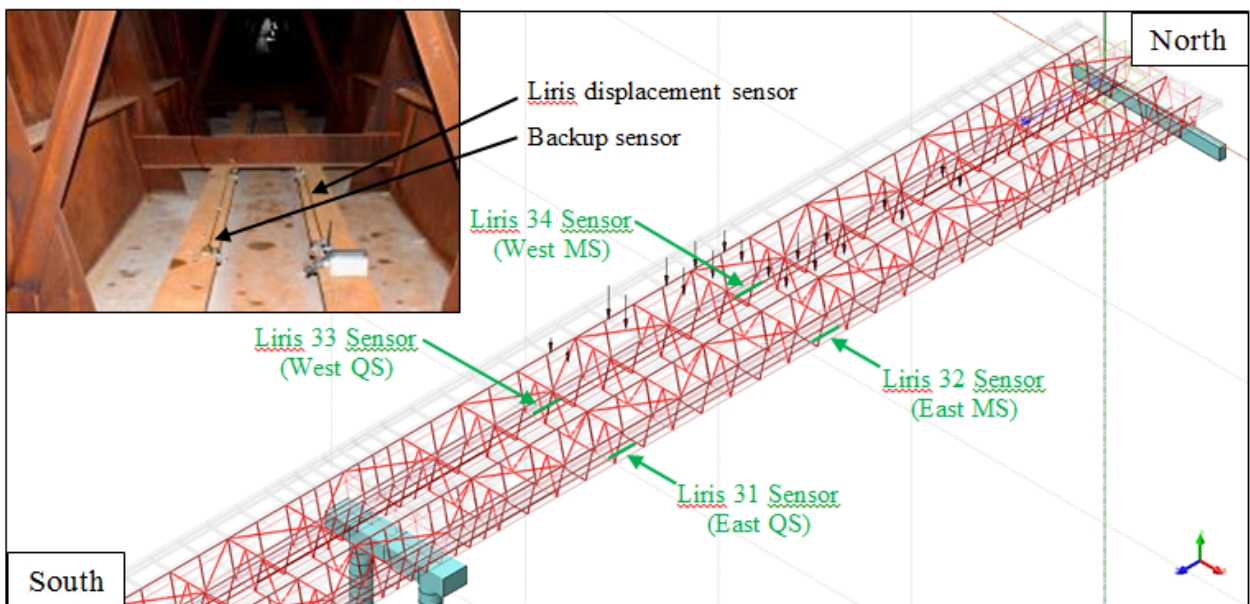


Fig 11: Detailed view of FE model showing locations of sensors (green arrows) and truck axle loads (black arrows)

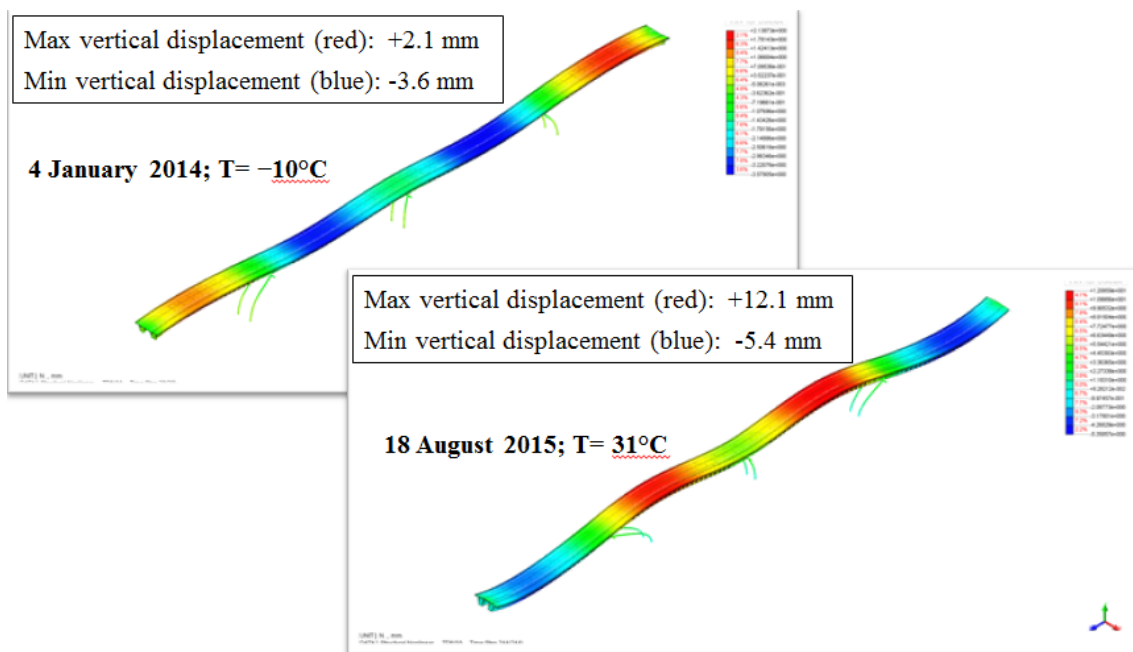


Fig 12: Simulated thermal deformations for a cold winter day (left) and a warm summer day (right)

4.2 Simulation of Thermal Deformation

Measured bridge temperatures (Figure 6) were used as input data in a structural nonlinear analysis of the bridge model, with time steps ranging from 0 day (2014-12-17) to 412 days (2016-02-02). For example, Figure 12 (left) above presents the thermal deformation (vertical displacement) of the bridge computed for January 14, 2014 corresponding to the satellite pass with the coldest temperature of the year. One can see the deck contraction towards the middle pier, producing inward bending of the two other piers, and bending of the concrete deck. Figure 12 (right) presents the thermal deformation (vertical displacement) of the bridge computed for August 18, 2015, corresponding to the satellite pass with the warmest temperature of the year. One can observe the elongation of the bridge deck away from the middle pier, producing an outward bending of the two other piers, and the bending of the concrete deck.

5. Validation of Satellite-Based Monitoring Technology

Movement obtained from InSAR analysis of satellite data represents the line-of-sight (LoS) movement, which is the change in the distance between the satellite and the point target being monitored on the ground (herein on a bridge). Since the satellite incidence angle is not 0° (from the vertical), detected movement includes horizontal and vertical components of unknown proportion to each other. For example, a positive LoS displacement (i.e. movement away from satellite) may be the result of a downward vertical displacement, a horizontal displacement away from satellite, or an unknown combination of both.

To allow comparison of SAR data with FEM data, it was decided to convert the FEM displacement data (knowing exactly the horizontal and vertical components) into LoS displacement (given the satellite viewing geometry) with the following equation:

$$\Delta LoS = -\Delta V (\cos \alpha \cos \gamma - \sin \alpha \sin \beta \sin \gamma) - \Delta H (\sin \alpha \sin \beta \cos \gamma - \cos \alpha \sin \gamma) \quad (1)$$

where ΔLoS is the line-of-sight displacement; ΔV is the vertical displacement; ΔH is the horizontal displacement; α is the incidence angle of the satellite line-of-sight direction (26.5° for SLA74-asc); β is the angle between the azimuth of satellite track on earth and the azimuth of bridge (26° between the SLA74-asc satellite track and the North Channel Bridge); and γ is the inclination angle of the bridge deck from North to South (1.2° for the North Channel Bridge).

An interesting special case for the above equation is when the bridge longitudinal direction is parallel to the satellite path (i.e. $\beta = 0^\circ$), in which case Eq. 1 would reduce to $\Delta LoS = -\Delta V \cos \alpha$. As a direct consequence, the sensibility of InSAR LoS measurements to any horizontal movement will be negligible. On the other hand, if β was 90° , the sensitivity to horizontal movement would be at its highest level.

Using Equation 1 above, the SAR displacement temperature sensitivity data can be compared directly to FEM thermal data when FEM data is expressed in terms of LoS displacement as a function of change in temperature from a reference temperature (set here as $T = 0^\circ\text{C}$). To that effect, these data were plotted in Figure 13 for 9 different positions on the bridge deck, being over vertical supports and mid-span locations. Two key observations can be made from Figure 13:

- A strong correlation exists between LoS displacement and temperature at any given location on the bridge;
- The slope of the linear regression analysis for each curve is a parameter that can be directly compared to the SAR line-of-sight displacement temperature sensitivity.

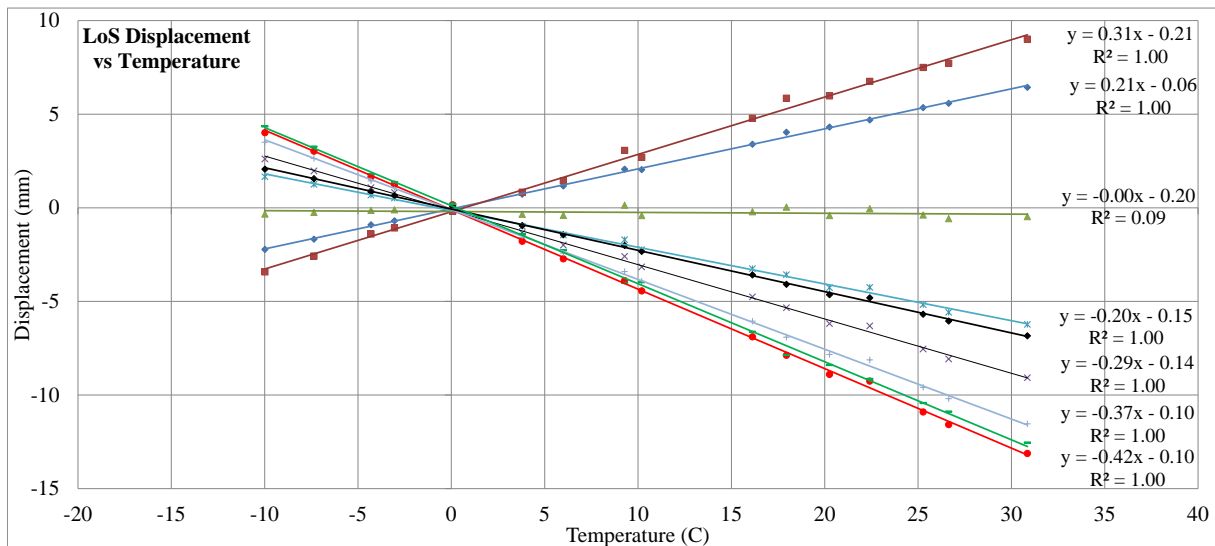


Fig. 13: FEM line-of-sight displacement correlated with temperature

The slopes of the linear regressions presented above were then expressed as the FEM thermal sensitivity along the longitudinal distance on the bridge, and illustrated in Figure 14. It is interesting to see how the thermal sensitivity varies along the bridge. Figure 14 also compares the two sets of independent SAR and FEM data, where a good fit can be observed. Note that there were not enough valid SAR point targets near the south end of the bridge to generate points for $x > 275$ meters. Longer monitoring, adding more valid PTs to the InSAR analysis, would eliminate this issue.

It is noted that the 2 peaks at approximately $x = 125$ m and 225 m appear more accentuated for the FEM data than for the SAR data. It was therefore suspected that the support conditions at the three piers could play a role and affect the thermal sensitivity of the FEM displacement data.

To investigate this further, the bridge model was modified to change the support conditions, i.e. to release the longitudinal movement of the connections of Piers 1 and 3 to the deck structure. In other words, unidirectional bearings were simulated in Piers 1 and 3, as opposed to the as-designed fixed connection. As shown in Figure 15, the two peaks appear to be flatter than with the previous support condition, and the correlation with the SAR data seems to have changed slightly. More monitoring and inspection data are required before concluding on the status of the support conditions.

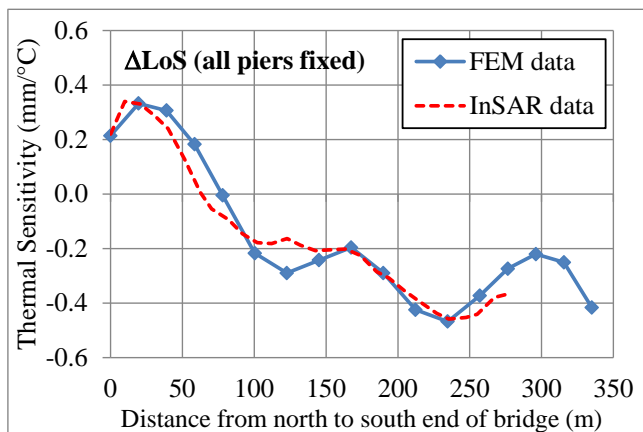


Figure 14: Comparison of FEM and SAR data sets for thermal sensitivity of line-of-sight displacement (for actual bridge support condition: all piers fixed)

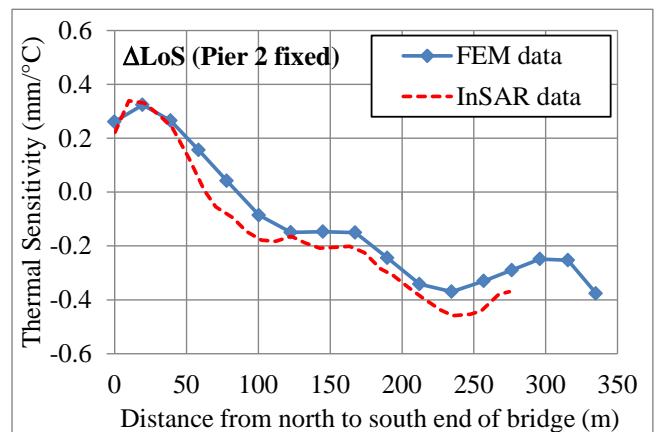


Figure 15: Comparison of FEM and SAR data sets for thermal sensitivity of line-of-sight displacement (for fictitious bridge support condition: only P2 fixed)

Nevertheless, an important point is made from the above discussion and illustrated data in Figures 14 and 15 that the SAR/FEM comparison of the LoS displacement thermal sensitivity data can be used to identify the following bridge issues:

- frozen or damaged bearings
- pier flexibility issues, or
- numerical modelling issue!

As mentioned above, our adopted approach is to use multi-model regression analysis to fit SAR satellite data against height and temperature in order to properly position point targets on the bridge, identify valid data points, and remove thermal movement in order to obtain the remaining residual dataset of displacement time rate, which represents the mechanical movement of the bridge that could be due to unexpected settlement, problematic joints or bearing, excessive loading, etc.

6. Conclusions

The key findings of this study are as follows:

- Regression analysis of SAR data from the satellite produced the best coherence when fitted against three independent variables: height, temperature, and time. For example, when temperature was excluded from the fit, the data coherence reduced significantly.
- The bridge railings appeared to be excellent SAR reflectors with their sharp edges and regular spacing along the bridge, returning over 3,000 clear signals to the satellite;
- The SAR displacement thermal sensitivity was found to compare well to FEM thermal data when computed along the longitudinal axis of the bridge. Such data was found promising, for example, to detect possible issues with problematic bearing conditions.
- Results show great promise and value in applying satellite-based technology for the remote monitoring of highway bridges to optimize preventive maintenance management, extend structural lifespan, minimize traffic disruptions due to late repairs, and ensure structural integrity after extreme events such as major earthquakes and flooding.

References

Cusson D, Ghuman P, Gara M & McCardle A 2012, "Remote Monitoring of Bridges from Space", *54th Annual Brazilian Congress on Concrete (IBRACON)*, October, 25 p.

Ferretti A, Monti-Guarnieri A, Prati C, Rocca F & Massonnet D 2007, "InSAR Principles: Guidelines for SAR Interferometry Processing and Interpretation", *ESA Publication TM-19*, February, 48 p.

Marinkovic P, Ketelaar G, Van Leijen F & Hanssen R 2007, "InSAR quality control - Analysis of five years of corner reflector time series", *5th International Workshop on ERS/Envisat SAR Interferometry (FRINGE07)*, Frascati, Italy, November, 5 p.

U.S. DOT, FHWA & FTA 2007 "The 2006 Status of the Nation's Highway Bridges and Transit: Conditions & Performance", *Report to Congress*.

Acknowledgments

Direct financial contribution to this project was provided by Transport Canada. Technical assistance and logistics were provided by National Research Council Canada, Federal Bridge Corporation Ltd., 3v Geomatics, Osmos Canada, Seaway Intl. Bridge Corporation, Morrison Hershfield, and Canadian Space Agency.